Coordination of 1,4-Diazabutadiene Ligands to Decamethylytterbocene: Additional Examples of Spin Coupling in Ytterbocene Complexes

Marc D. Walter, David J. Berg and Richard A. Andersen*

Department of Chemistry and Chemical Sciences Division of Lawrence Berkeley National Laboratory,

University of California, Berkeley, California, CA 94720

E-mail: raandersen@lbl.gov

Address correspondence to this author at Department of Chemistry, University of California, Berkeley,

CA 94720. E-mail: raandersen@lbl.gov

Abstract

The paramagnetic 1:1 coordination complexes of $(C_5Me_5)_2Yb$ with a series of diazabutadiene ligands, $RN=C(R')C(R')=NR$, where R= CMe_3, $CHMe_2$, adamantyl, *p*-tolyl, *p*-anisyl, and mesityl when R'=H, and R= *p*-anisyl when R'= Me, have been prepared. The complexes are paramagnetic, but their magnetic moments are less than expected for the two uncoupled spin carriers, $(C_5Me_5)_2Yb(III, 4f^{13})$ and the diazabutadiene radical anions (S= ½), which implies exchange coupling between the spins. The variable temperature ^{1}H NMR spectra show that rotation about the R-N bond is hindered and these barriers are estimated. The barriers are largely determined by steric effects but electronic effects are not unimportant.

1

Introduction

Coordination complexes of the type $Cp'_2Yb(bipy-X)$, where Cp' is a substituted cyclopentadienyl ligand and bipy-X is a 4,4'-disubstituted bipyridine ligand, are molecules in which the bipyridine ligand is a radical anion.[1-3] However, the magnetic moments in these complexes are lower than expected, which implies that the spin carriers are coupled, that is, the spin on the $[Cp'_2Yb(III, 4f^{13})]$ fragment is coupled with the spin on the bipy-X radical anion (S= ½) fragment. Although the spin carriers are antiferromagnetically coupled, the mechanism by which they couple is not clear; the coupling mechanism is important since exchange coupling between f-electrons with paired electrons or with other f-electrons is generally weak.[4, 5] The magnetic moments of the ytterbocene-bipy complexes range from small, where $\mu_{eff} \approx 0.7 \mu_B$, to large, where $\mu_{eff} \approx 3.3 \mu_B$ at 300 K, depending on the substituents on the ligands, which implies that the exchange coupling is strong.[1-3] The terpyridine and substituted terpyridine complexes of decamethylytterbocene behave similarly.[6, 7] The implication of strong antiferromagnetic coupling in these ytterbocene-bipy complexes provides new ways of thinking about the specific role that electrons in f-orbitals play in bonding in these particular complexes, where an unpaired electron resides in a ligand molecular orbital, which is related to the concept of covalence in f-element compounds in general.[8]

This paper continues our phenomenological studies of exchange coupling in decamethylytterbocene complexes by preparing the 1,4-diazabutadiene complexes $(C_5Me_5)_2Yb(RN=C(R')C(R')=NR)$, where R is an alkyl ($Me_3C$, Me_2HC and adamantyl) or aryl (*p*-tolyl, *p*-anisyl and mesityl) group and R' is either H or Me, abbreviated $Cp*_2Yb(dad(R')-R)$. Several diazabutadiene complexes of lanthanide metallocenes have been described for Sm^9, Eu^{10} and Yb.[11-14] However, the reactions of $(indenyl)_2Yb(thf)_2$ and $(fluorenyl)_2Yb(thf)_2$ with aryl substituted 1,4-diazabutadiene do not yield simple metallocene adducts, but complexes derived from C-C coupling and C-H bond activation are observed.[15, 16]

Results and Discussion

Comparison Between bipy and dad(R')-R Ligands

The frontier molecular orbitals of bipy[17, 18] and dad(H)-R[19] are isolobal. The sigma donor orbitals on each nitrogen atom of bipy and dad(H)-R transform as a_1+b_2 (in C_{2v} symmetry). The LUMO is of b_1 symmetry (in C_{2v} symmetry) in each case as illustrated in **A** and **B**. The energy of the LUMO is measured by the reduction potential of the neutral ligands. The reduction potential of some of the 1,4-diazabutadiene ligands used in this study are listed in Table 1; the value for bipy is listed for comparison.
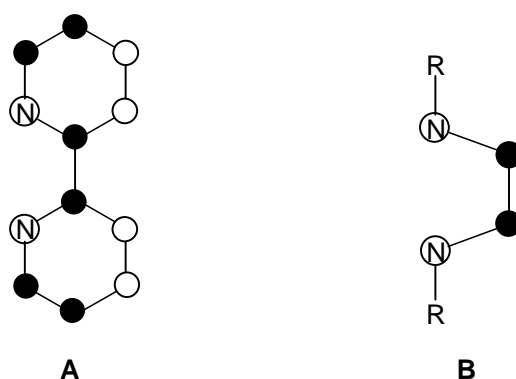

A   **B**

**Table 1.** Reduction potentials of 1,4-diazabutadiene (dad(R')-R) ligands[20, 21]

R'	R	$E_{1/2}(L^{0/-})^a$ / V
H	CMe$_3$	-2.13
H	*p*-tolyl	-1.40
H	*p*-anisyl	-1.47
Me	*p*-anisyl	-1.85
bipy		-2.12

[a] Potentials quoted relative to SCE in 0.1 M [^{n}Bu$_4$N][BF$_4$]-DMF at 293 K.

The reduction potentials show that the LUMO is lower in energy for the dad(H)-R ligands when R is a substituted benzene group relative to bipy, but when R is CMe$_3$, the energy of the LUMO is essentially

3

the same as that of bipy. Substituent effects change the reduction potential by 0.73 V,[20, 21] and these changes are readily rationalized by inductive and resonance effects when the substituents on the nitrogen atoms are aromatic rings and by hyperconjugation when the substituents are alkyl groups. Since the diazabutadiene ligands are as easy or easier to reduce than bipy, they are generally thought to be better π-acceptors.[22]

Synthesis and Physical Properties. All of the dad(R')-R complexes are prepared by adding the diazabutadiene ligand to $(C_5Me_5)_2Yb(OEt_2)$ in hydrocarbon solvent at room temperature, eq.1. The 1:1 complexes are either green or red in color and most of them are difficult to purify by crystallization from the mother liquor. However, most sublime in the temperature range 160-220 °C in diffusion pump vacuum and the sublimed compounds readily crystallize from pentane or toluene solution. The pure complexes are high melting solids, and those that sublime yield molecular ions in their mass spectra; these and other physical properties are shown in Table 2.

$$(C_5Me_5)_2Yb(OEt_2) + dad(R')-R \xrightarrow{\text{toluene}} (C_5Me_5)_2Yb(dad(R')-R) + OEt_2 \qquad (1)$$
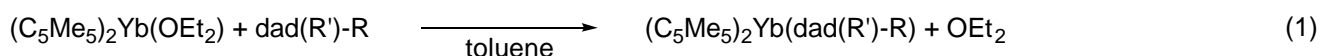
R'	R	abbreviation
H	C(Me)$_3$	dad(H)-*t*-Bu
H	CH(Me)$_2$	dad(H)-*i*-Pr
H	adamantyl	dad(H)-adamantyl
H	C$_6$H$_4$-*p*-Me	dad(H)-*p*-tolyl
H	C$_6$H$_4$-*p*-OMe	dad(H)-*p*-anisyl
H	C$_6$H$_2$-2,4,6-(Me)$_3$	dad(H)-mesityl
Me	C$_6$H$_4$-*p*-OMe	dad(Me)-*p*-anisyl

4

Table 2. Solid state properties of ytterbocene 1,4-diazabutadiene complexes

Compound	color	mp/°C	IR[a]/cm^{-1}	$\mu_{eff}(300K)$[b]/μ_B
$(C_5Me_5)_2Yb(dad(H)$-p-tolyl)	green	220 (dec.)	313	3.97
$(C_5Me_5)_2Yb(dad(H)$-p-anisyl)	red	260-262 (dec.)	308	3.72
$(C_5Me_5)_2Yb(dad(Me)$-p-anisyl)	green-brown	219-221	295	3.96
$(C_5Me_5)_2Yb(dad(H)$-mesityl)	blue-green	230-232 (dec.)	-	-
$(C_5Me_5)_2Yb(dad(H)$-t-Bu)	red	220-222 (dec.)	280	3.63
$(C_5Me_5)_2Yb(dad(H)$-i-Pr)	red	208-211 (dec.)	295	3.71
$(C_5Me_5)_2Yb(dad(H)$-adamantyl)	brown-red	238-239	280	3.43
$(C_5Me_4H)_2Yb(dad(H)$-t-Bu)	red	242-245 (dec.)	-	-
$(C_5H_5)_2Yb(dad(H)$-t-Bu)[11]	yellow	-	-	3.34

[a] Ytterbium-C_5Me_5 ring symmetric tilting frequency (ref. 4). [b] Determined from a plot of χT vs. T, where $\mu_{eff}= 2.828 (\chi T)^{0.5}$ and T= 300 K.

The infrared spectra in the low energy region show an absorption that is associated with the $(C_5Me_5)_2Yb(III)$ fragment, Table 2.[4] The solution ^1H NMR chemical shifts at 20 °C are indicative of paramagnetic complexes, as are their temperature dependence, see Table 5, below. All of the complexes are paramagnetic in the solid state but their μ_{eff} values, which lie in the narrow range between 3.3 and 4.0 μ_B at 300 K, are lower than expected; the expected value for the two uncoupled spin carriers, $Cp'_2Yb(III, 4f^{13})$ and a diazabutadiene radical anion (S= ½), is 4.85 μ_B.[23] The lowered value of μ_B implies that the spin carriers are antiferromagnetically coupled as in the bipy-X complexes. However, the temperature dependence of the magnetic susceptibility is not simple antiferromagnetic coupling between the spin carriers, which is also true for the bipy-X complexes; these details are described below.[1-3, 8]

Solid State Crystal Structures. The ORTEP diagrams for two representative molecules, $(C_5Me_5)_2Yb(dad(H)-R)$, where R= *p*-tolyl and *p*-anisyl, are shown in Figures 1 and 2. The crystal data and packing diagrams are available as Supporting Information. Bond distances and angles for these two complexes are given in Table 3 and 4 along with data for related ytterbocene diazabutadiene complexes.[11, 12]
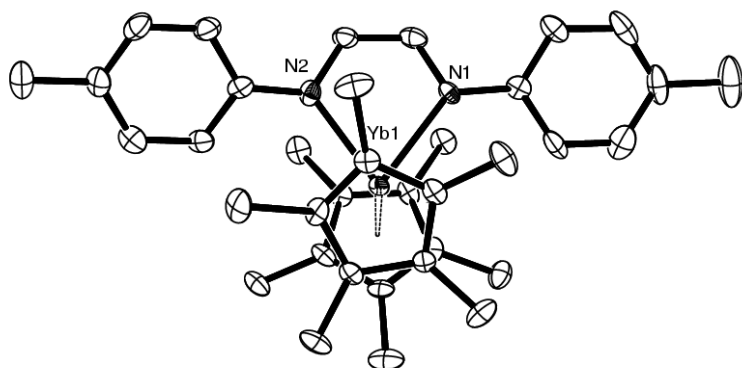

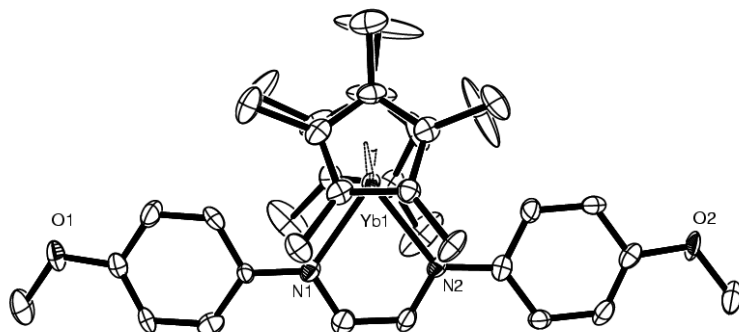**Figure 1.** ORTEP diagram of $(C_5Me_5)_2Yb(dad(H)-p$-tolyl) (50 % probability ellipsoids).

Figure 2. ORTEP diagram of $(C_5Me_5)_2Yb(dad(H)-p$-anisyl) (50 % probability ellipsoids).

The two complexes shown in Figures 1 and 2 have approximate C_{2v} symmetry and the C_5Me_5 rings are staggered in the *p*-tolyl derivative but eclipsed in the *p*-anisyl derivative. The NCCN atoms in the diazabutadiene ligands are planar since their torsion angles are 0.5° in each complex. The averaged

6

value of the angle formed by the intersection of the planar *p*-tolyl ring [NC(ipso)C(ortho)C(ortho)] and the NCCN plane is 21.5° in $(C_5Me_5)_2Yb(dad(H)$-*p*-tolyl); in the *p*-anisyl complex this angle is 4.5°. This difference could be due to different intramolecular steric effects between the N-Ar fragment and the orientation of the C_5Me_5 rings in the solid state. That is, the steric interaction is minimized when the C_5Me_5 rings are eclipsed and the NAr fragments are nearly coplanar with the NCCN fragment, which maximizes the extent of N-C(ipso) π-bonding.

The averaged Yb-C and Yb-N distances in both molecules are statistically equal as are the Cp(ring centroid)-Yb-Cp(ring centroid) angles. The distances are in the range expected for a $(C_5Me_5)_2Yb(III)$ fragment and similar to those found in the dad(H)-*t*-Bu complexes (Table 3).[11, 12] These values may be compared to the Yb-C and Yb-N distances in $(C_5Me_5)_2Yb(py)_2$ of 2.74 Å and 2.56 Å, respectively,[24] both of which are significantly longer than the comparable distances for the complexes given in Table 3. In addition, the Yb-N distance in $(C_5H_5)_2Yb(dad(H)$-*t*-Bu) is significantly shorter than that in $(C_5Me_5)_2Yb(dad(H)$-*t*-Bu), which is consistent with intramolecular steric effects.[12]

Table 3. Selected Bond Distances (Å) and Angles (°) of $(C_5H_5)_2Yb(dad(H)$-*t*-Bu),[11] $(C_5Me_5)_2Yb(dad(H)$-*t*-Bu),[12] $(C_5Me_5)_2Yb(dad(H)$-*p*-tolyl) and $(C_5Me_5)_2Yb(dad(H)$-*p*-anisyl).

	$(C_5H_5)_2Yb$ (dad(H)-*t*-Bu)[a]	$(C_5Me_5)_2Yb$ (dad(H)-*t*-Bu)[b]	$(C_5Me_5)_2Yb$ (dad(H)-*p*-tolyl)[c]	$(C_5Me_5)_2Yb$ (dad(H)-*p*-anisyl)[c]
Yb-C$_{ring}$ (mean)	2.60	2.69	2.65	2.64
Yb-C$_{ring}$ (range)	2.585(14)- 2.610(14)	2.656(3)- 2.716(1)	2.623(6)- 2.683(6)	2.623(9)- 2.658(9)
Yb-centroid	2.33, 2.33	2.41; 2.40	2.37; 2.34	2.36; 2.35
centroid-Yb- centroid	128	130	137	139
Yb-N	2.306(9); 2.306(9)	2.385(3); 2.394(3)	2.340(5); 2.368(5)	2.339(7); 2.337(6)
N-Yb-N	74.7(3)	75.3(1)	73.4(2)	72.5(2)

R-N-C (ave.)	117.0	113.3	118.3	119.5

[a] From ref. 11. [b] From ref. 12. [c] This work.

The bond distances in the dad(H)-R fragments support the view that it is a radical anion. The uncoordinated diazabutadiene dad(H)-t-Bu, in the trans-conformation, has been structurally characterized.[25] The data in Table 4 compare the C-C and C-N bond distances in the four ytterbocene complexes with those in the free diazabutadiene. The C-C distances shorten and the C-N distances lengthen in the complexes relative to the distances in the free ligand, as expected when the LUMO of the diazabutadiene illustrated in **B**, above, is populated. The crystallographic data and all of the other data clearly support the idea that the complexes are derived from radical anions and cationic ytterbocene fragments.

Table 4. Bond Distances (Å) in Diazabutadiene Ligands from X-ray Crystallography

	free dad(H)-tBu [a]	$(C_5Me_5)_2Yb$ (dad(H)-t-Bu) [b]	$(C_5H_5)_2Yb$ (dad(H)-t-Bu) [c]	$(C_5Me_5)_2Yb$ (dad(H)-p-tolyl) [d]	$(C_5Me_5)_2Yb$ (dad(H)-p-anisyl) [d]
A	1.467(2)	1.398(3)	1.398(10)	1.380(9)	1.382(13)
B	1.267(2)	1.339(2)	1.299(10)	1.342(8)	1.335(11)
C	1.267(2)	1.326(5)	1.310(10)	1.342(8)	1.339(11)

[a] From ref. 25. [b] From ref. 12. [c] From ref. 11. [d] This work.
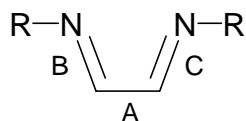

Figure for Table 4

Solid State Magnetic Measurements. The magnetic susceptibility measurements as a function of temperature provide a bulk measure of how the paramagnetic condition changes with temperature. A plot of χ^{-1} as a function of temperature for all the complexes is shown in Figure 3 and a plot of μ_{eff} vs. T

for some of them is shown in Figures 4a and 4b. The χT vs. T plots are available as Supporting

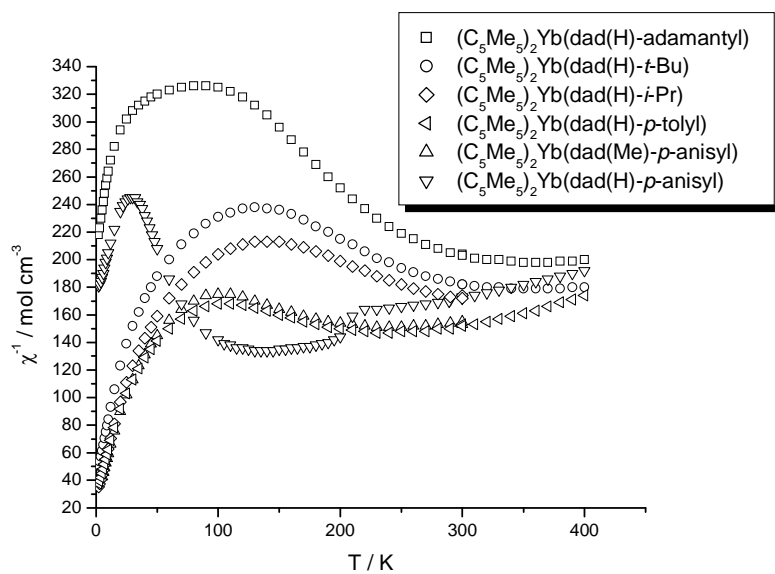Information.

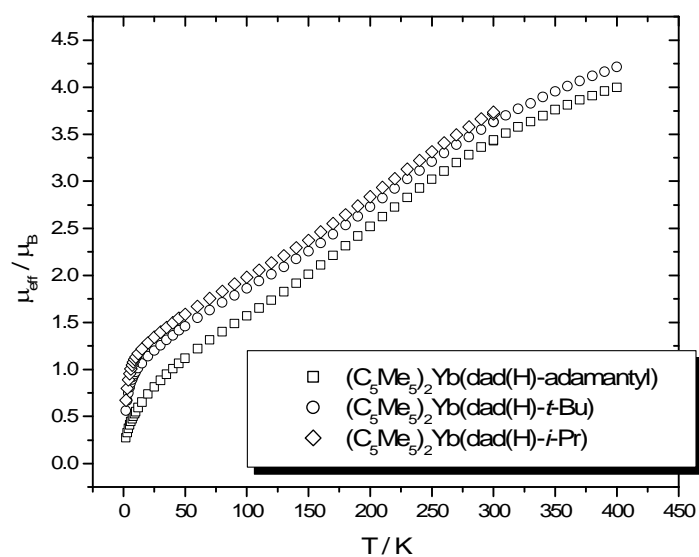**Figure 3.** χ^{-1} vs. T plot of $(C_5Me_5)_2Yb(dad(R')-R)$ compounds

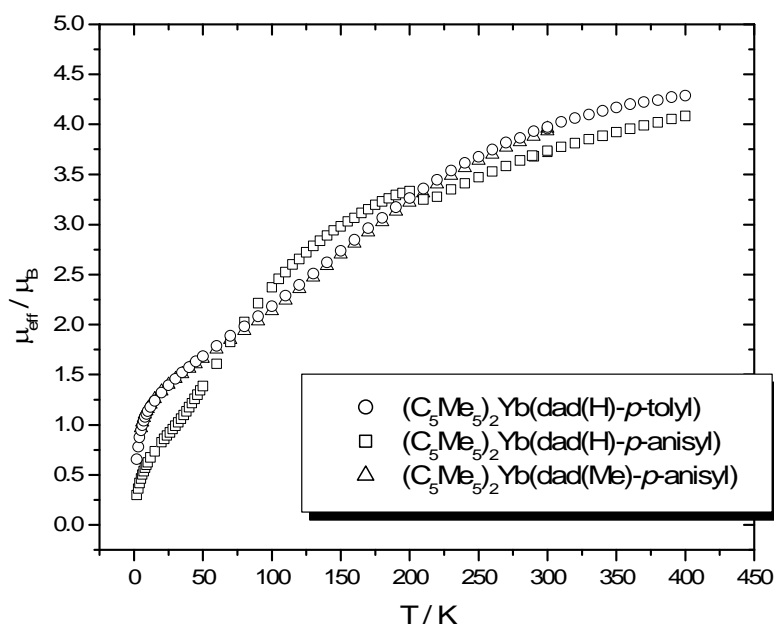**Figure 4a.** μ_{eff} vs. T plot of $(C_5Me_5)_2Yb(dad(H)-alkyl)$ compounds

Figure 4b. μ_{eff} vs. T plot of $(C_5Me_5)_2Yb(dad(R')-aryl)$ compounds

The plots of χ^{-1} vs. T and μ_{eff} vs. T define a family of curves, with one exception, in which μ_{eff} increases, more or less smoothly, to 400 K, where the curves appear to saturate with an effective magnetic moment of 3.9-4.2 μ_B. These plots are similar in shape to those for the bipy-X derivatives, though the net magnetic moments in the high temperature regime are much lower, in the range of 1-3.9 μ_B (at 400 K).[1-3] This pattern implies that the reason for the lowered magnetic moments, relative to the value expected for two uncoupled spin carriers, is the same, *viz.*, exchange coupling between the unpaired electron in the $(C_5Me_5)_2Yb(III)$ fragment with the electron in the b_1 symmetry orbital of the ligand. The extent of coupling and therefore the coupling constant depends upon several variables, the principle ones being the overlap between and the relative energy of the magnetic orbitals.[3] Detailed studies similar to those published in ref. 8 are underway to make this qualitative statement more quantitative. Recent articles claim that the variation in the magnetic moment as a function of temperature is due to a tautomeric equilibrium between the diamagnetic $[(C_5Me_5)_2Yb(II, 4f^{14})(bipy, S= 0)]$ spin isomer and the paramagnetic $[(C_5Me_5)_2Yb(III, 4f^{13})(bipy^{\bullet-}, S= \frac{1}{2})]$ spin isomer.[6, 26] This

explanation is incorrect for $(C_5Me_5)_2Yb(bipy)$ since the shape and therefore the population of Yb(II) and Yb(III) signatures in the Yb L_{III}-edge XANES do not change from 10 to 400 K.[8, 27]

The one exception to the generalizations mentioned above is the χ^{-1} vs. T plot for $(C_5Me_5)_2Yb(dad(H)$-*p*-anisyl). Although the plot is qualitatively similar to that of $(C_5Me_5)_2Yb(dad(Me)$-*p*-anisyl), Figure 5, the slope of χ^{-1} vs. T for the former complex increases much more rapidly with temperature, passing through a sharp maximum at ≈ 25 K, then decreases much more rapidly than in the other complexes. About 200 K, a sudden increase occurs over the temperature range of 15 K, before the χ^{-1} value approaches that found for the other complexes. The origin of the difference in the solid state magnetic behavior of these two molecules is unknown.
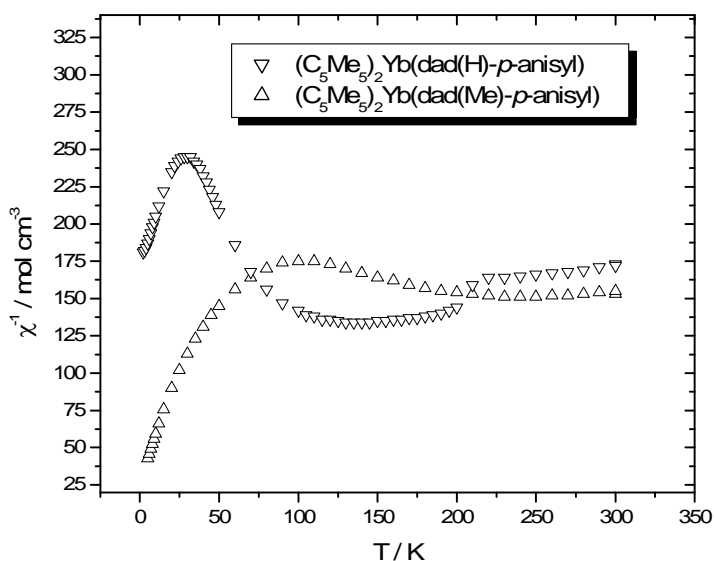

Figure 5. χ^{-1} vs. T plot of $(C_5Me_5)_2Yb(dad(H)$-*p*-anisyl) and $(C_5Me_5)_2Yb(dad(Me)$-*p*-anisyl)

Figure 6 shows a χ^{-1} vs. T plot for $(C_5H_5)_2Yb(dad(H)$-*t*-Bu) and $(C_5Me_5)_2Yb(dad(H)$-*t*-Bu). As the curves are nearly superimposible, the substituents on the cyclopentadienyl ligand do not appreciably

change the magnetic moment. This is unlike the behavior of the bipyridine complexes where the effective magnetic moments depend upon the substituents on the cyclopentadienyl ring.[1, 2]
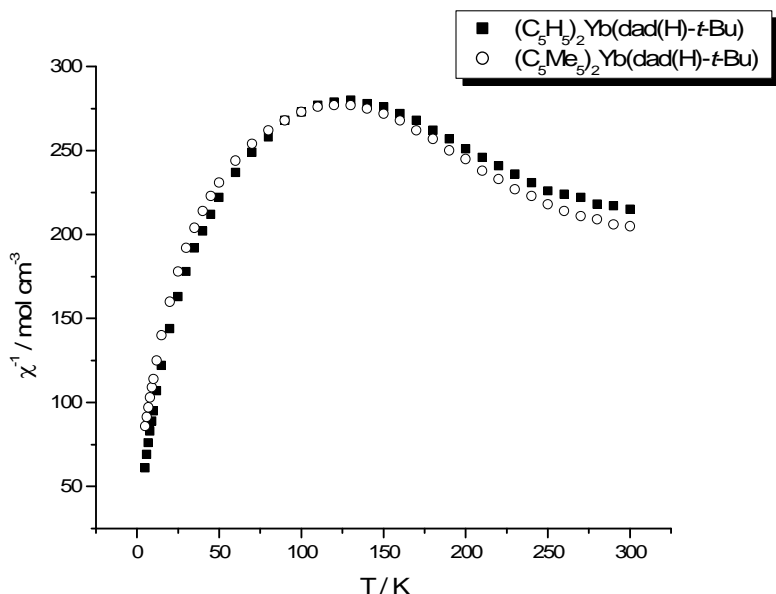

Figure 6. χ^{-1} vs. T plot of $(C_5Me_5)_2Yb(dad(H)-t-Bu)$ and $(C_5H_5)_2Yb(dad(H)-t-Bu)$

Solution ^{1}H NMR Spectroscopic Studies. (a) General.

The observed solution ^{1}H NMR chemical shifts in C_6D_6 at 20 °C for the complexes described in this paper are listed in Table 5.[28] In general, the chemical shifts of the C_5Me_5 groups are relatively broad and lie in a narrow chemical shift range from $\delta= 2.8$ to 0.15 ppm. The resonances due to the diazabutadiene ligands vary widely in chemical shift and line width. Since assignments can be made on the basis of relative intensities, and in some cases specific substitutions, some generalizations can be made. The backbone CH's appear upfield in the chemical shift range of $\delta= -25$ to -146 ppm with the most shielded resonances associated with the dad(H)-R ligands in which R is a substituted benzene ring. When R is an alkyl group the resonances appear in a very narrow range, $\delta= -25$ to -28 ppm. The chemical shift of the *meta*-CH groups of the substituted benzene ring are observed in the range $\delta= +47$ to $+62$ ppm, but the *ortho*-H's are observed in only one case. These chemical shift values clearly show

12

that the complexes are paramagnetic in solution. In these complexes coordinated diazabutadiene ligand does not exchange with added free diazabutadiene ligand over the temperature range of −80 to +90 °C, showing that the dynamic processes, described in detail below, are due to intramolecular processes.

Table 5. ^{1}H NMR Data for Cp'$_2$Yb(dad(R')-R) Complexes

Compound	Cp'	R'	R	
(C$_5$Me$_5$)$_2$Yb(dad(H)-*p*-tolyl)	1.74 (35)	-123.7 (320)	*o*-CH	a)
			m-CH	50.2 (700)
			p-Me	58.3 (90)
(C$_5$Me$_5$)$_2$Yb(dad(H)-*p*-anisyl)	1.76 (13)	-109.3 (270)	*o*-CH	a)
			m-CH	46.9 (350)
			p-OMe	18.9 (4)
(C$_5$Me$_5$)$_2$Yb(dad(Me)-*p*-anisyl)	1.51 (23)	+126.0 (360)	*o*-CH	103.3 (800)
			m-CH	50.1 (34)
			p-OMe	18.5 (8)
(C$_5$Me$_5$)$_2$Yb(dad(H)-mesityl)	0.29 (90)	-146.2 (240)	*o*-CH$_3$	224.9 (120)
			o-CH$_3$	58.2 (64)
			m-CH	62.5 (32)
			m-CH	50.4 (24)
			p-Me	58.2 (64)
(C$_5$Me$_5$)$_2$Yb(dad(H)-*t*-Bu)	0.15 (8)	-26.6 (200)	*t*-Bu	a)
(C$_5$Me$_5$)$_2$Yb(dad(H)-*i*-Pr)	2.83 (9)	-28.3 (170)	CH	108.9 (260)
			Me	32.3 (12)
(C$_5$Me$_5$)$_2$Yb(dad(H)-adamantyl)	0.14 (8)	-25.2 (200)	CH$_2$	18.9 (650)
			CH$_2$	16.7 (400)
			CH	12.5 (67)
(C$_5$Me$_4$H)$_2$Yb(dad(H)-*t*-Bu)	Me 2.62 (34)	-36.0 (180)	*t*-Bu	42.7 (480)
	Me 2.47 (50)			

	H	-38.0 (60)			
(C$_5$H$_5$)$_2$Yb(dad(H)-t-Bu)	-23.8 (60)		-42.5 (208)	t-Bu	45.8 (46)

Recorded in benzene-d_6 at 20 °C. Observed chemical shifts are given in ppm. Line widths, full width at half height (Hz), are given in parentheses. [a] These resonances are not observed at 20 °C.

In this and earlier papers, variable temperature ^{1}H NMR spectroscopy is used as a probe of dynamic processes in solution. Plots of δ vs. T^{-1} indicate if intramolecular exchange is occurring on the NMR time scale and if the chemical shifts are linear in T^{-1}. In order to ensure that all intermolecular processes are slow on the NMR time scale, generally, variable temperature data in the presence and absence of added exchangeable ligand are obtained.[1-3] In the best experiments, coalescence-decoalescence behavior is observed from which $\Delta G^{\ddagger}(T_c)$ is obtained and a physical process responsible for the fluxionality is generally obvious.[29, 30]

When the δ vs. T^{-1} plots are non-linear, there is insufficient information in the line-shape to postulate a physical process other than some intramolecular process(es) occurring in solution is(are) temperature dependent. A physical process that changes the populations will give rise to the resonances that have non-linear dependence on T^{-1}, e.g. geometric changes, intramolecular fluxions, electronic exchange, etc.[31-33] In general, our interest is to obtain $\Delta G^{\ddagger}(T_c)$ for chemical exchange process, and the issue of non-linearity is not addressed. However, the bipy and related N-heterocyclic complexes present a new challenge since these ligands in these complexes are radical anions and the effect of electron transfer, spin delocalization and/or exchange coupling on the line shape must be addressed in a realistic manner. A corollary is the origin of chemical shifts; we have not dealt explicitly with them until recently,[3] since we have simply viewed them as a number. For lanthanide molecules with neutral or anionic ligands, that are diamagnetic, the paramagnetic(isotropic) shifts are mainly due to the pseudo-contact term, $\delta^{pc} = -$ **D** G(θ, r), where **D** is the magnetic susceptibility tensor and G(θ, r) is the geometric term which is related to $\left\langle \dfrac{3\cos^2\theta - 1}{r^3} \right\rangle$, when axial symmetry is present.[31] Thus the isotropic chemical shift depends on the

14

distance r of the observed nucleus from the paramagnetic center (that is, the distance from the unpaired spin) and **D**, which is related to T^{-1}, if the Curie-law is followed. This is a good approximation for the vast number of complexes we have prepared over the years since the metal to ligand bonds are not covalent, that is, the unpaired spin density on the ligands is small since unpaired f-electrons are localized on the metal center and contributions from the Fermi contact term or deviations from the Curie-law to the overall isotropic chemical shift are small. We have recently shown that complexes in which the ligand is a radical anion, such as Cp'$_2$Yb(bipy-X), the plot of the solid state magnetic susceptibility, χT, vs. δ is linear for the 6,6'-H chemical shift at 300 K.[3] This is not surprising since the 6,6'-position carries a small amount of spin-density in the bipy-radical anion,[18] it is close to the paramagnetic center and the chemical shift should depend on the pseudo-contact contribution. For the other resonances that carry higher spin densities and are further away from the paramagnetic center, the Fermi contact term, δ^{Fc} is proportional to $- a_i \langle S \rangle_{av}$, where a_i is the isotropic hyperfine splitting constant and $\langle S \rangle_{av}$ is the thermal average of the spin moments along the principal molecular axes, which is related to the atomic magnetic susceptibility, will play a role.[34, 35] This term is an important contributor to the chemical shift when spin density is located on the ligand, *i.e.* when there is covalence and/or when the ligand is a radical anion as in the case of Cp'$_2$Yb(N-heterocyclic bases). Both Fermi contact and pseudo-contact terms are related to the magnetic susceptibility, and δ vs. T^{-1} plots are expected to be linear, if Curie-behavior is followed and if the isotopic chemical shifts account for *all* of the intramolecular dynamic processes.

(b) The Aryl Substituted Complexes, (C$_5$Me$_5$)$_2$Yb(dad(H)-R), R= aryl

The ^{1}H NMR data are shown as δ vs. T^{-1} plots, where δ is the observed chemical shift as in earlier papers.[1-3] An alternative method of representing the data is to plot the reduced chemical shift (ϑ_{298}) (the chemical shift at a given temperature multiplied by that temperature, δT divided by 298 K in order to get convenient numbers) as a function of T.[32, 36, 37] The latter representations are useful since they show the

relation between solid state magnetic susceptibility as a function of temperature when plotted as χT vs. T and the reduced chemical shift of a given resonance as a function of temperature, ϑ_{298} vs. T.[38, 39] These plots are available as Supporting Information.

The variable temperature ^{1}H NMR spectra of the *p*-tolyl and *p*-anisyl complexes are similar, and only δ vs. T^{-1} plots are shown for the *p*-tolyl complex in Figures 7a and 7b; the δ vs. T^{-1} plot for the *p*-anisyl complex is available as Supporting Information.
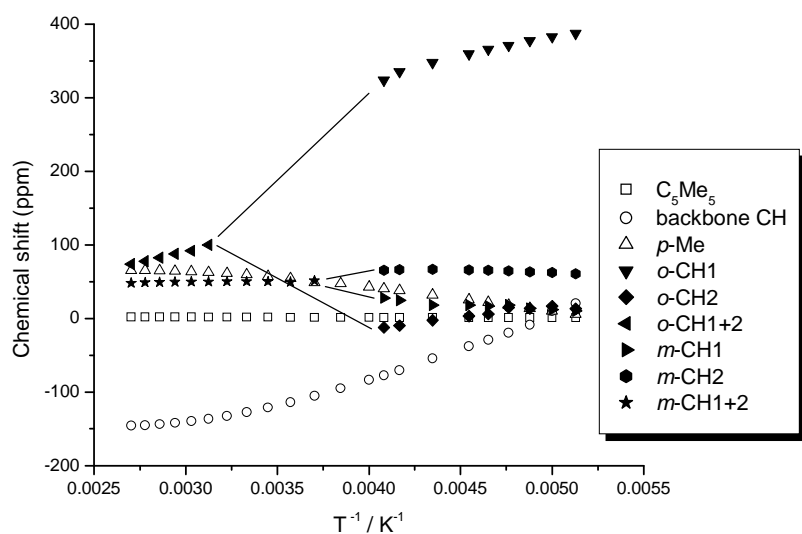

Figure 7a. Chemical shift (δ) vs. T^{-1} plot of the ^{1}H NMR resonances of (C$_5$Me$_5$)$_2$Yb(dad(H)-*p*-tolyl) in toluene-d_8 at temperatures from -70 to +90°C.
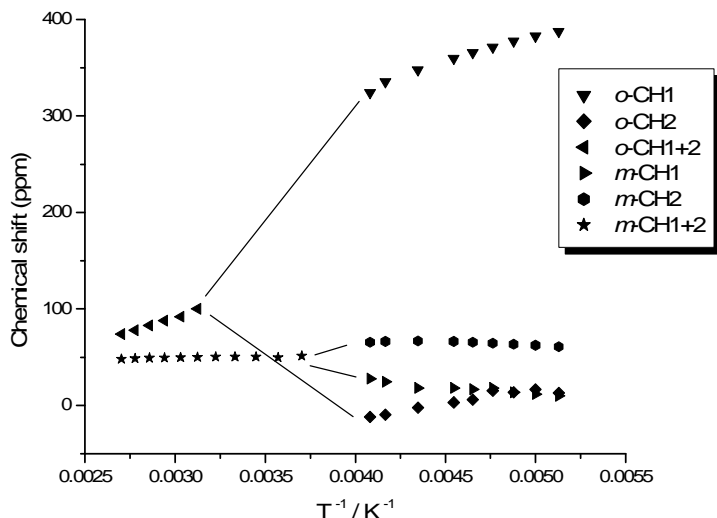
Figure 7b. Chemical shift (δ) vs. T^{-1} plot of the *ortho*-CH and *meta*-CH ^{1}H NMR resonances of $(C_5Me_5)_2Yb(dad(H)$-*p*-tolyl) in toluene-d_8 at temperatures from -70 to +90°C.

The C_5Me_5 resonances are essentially independent of temperature, though the *p*-Me and backbone CH resonances have a non-linear dependence on temperature. The resonances attributable to the benzene-ring *meta*- and *ortho*-CH's address the question of arene ring rotation in solution. At 20 °C, a single resonance of relative intensity 4H is observed, which broadens, disappears, then reappears as two resonances of 2H each as the temperature is decreased to −70 °C, Figure 7b. The coalesced resonance sharpens and the chemical shift is essentially independent of temperature from +20 °C to +90 °C. During the temperature study, another resonance that is very broad at 20 °C emerges from the baseline as the temperature is decreased as two widely separated resonances due to 2H each. As the temperature is increased from +20 °C to +90 °C, this coalesced resonance, due to 4H, is linear in temperature. These resonances are either the *ortho*- or *meta*-CH's and it is difficult to assign them with certainty, however, the broader one at 20 °C is likely to be the *ortho*-CH, since it is closer to the paramagnetic center. The assignment is not crucial, since the activation free energy derived from the line shape for both resonances is identical, Table 6. The temperature behavior of the resonances is as expected for hindered rotation of the *p*-tolyl group about the N-C(ipso) bond. At low temperature the two *p*-tolyl rings are orientated as in the solid state structure, Figure 1 and 2, the molecule has averaged C_{2v} symmetry and

17

each *ortho*- and *meta*-CH's are distal and proximal relative to the ytterbocene fragment. As the temperature is increased, rotation around the N-*p*-tolyl bond increases, resulting in distal-proximal site exchange with barriers of about 10 kcal mol^{-1} in each case, Table 6.

Table 6. Barrier of *ortho*-CH and *meta*-CH site exchange in $(C_5Me_5)_2Yb(dad(H)$-*p*-tolyl) and $(C_5Me_5)_2Yb(dad(H)$-*p*-anisyl)

	$(C_5Me_5)_2Yb(dad(H)$-*p*-tolyl)		$(C_5Me_5)_2Yb(dad(H)$-*p*-anisyl)	
	o-H	*m*-H	*o*-H	*m*-H
$\Delta\nu$ [Hz] [a]	12400	16800	85200	520
T_c [K] [b]	310	270	290	220
k_c [s^{-1}]	27546	37320	189266	1155
$\Delta G^{\ddagger}$ [kcal mol^{-1}] [c]	10.5	10.1	10.0	9.7

[a] Signal separation in Hz

[b] coalesence temperature (T_c) at 400 MHz operating frequency

[c] The free energy of activation, $\Delta G^{\ddagger}$, was determined by the temperature dependence of the *ortho*-CH and *meta*-CH proton resonances in C_7D_8 as outlined in ref. 40-42

The ^{1}H NMR spectrum of the mesityl complex, $(C_5Me_5)_2Yb(dad(H)$-mesityl), is useful since it provides an assignment of the *meta*-CH resonances and shows the effect of steric hindrance on the rotation barrier. The ^{1}H NMR spectrum shows two inequivalent *ortho*-Me and *meta*-CH resonances at +80 °C, Figure 8. These inequivalent *ortho*-CMe and *meta*-CH resonances are attributable to slow distal-proximal site exchange that is observed in the *p*-tolyl and *p*-anisyl complexes only at low temperature. Even though distal-proximal site exchange is slow at 80 °C, the mesityl complex has averaged C_{2v} symmetry since the C_5Me_5-rings are equivalent. As the temperature is lowered the C_5Me_5 rings become inequivalent, $\Delta G^{\ddagger}(T_c= 260 \text{ K}) = 11$ kcal mol^{-1}. Since the distal and proximal CMe and CH groups are still pairwise equivalent, the complex contains a time-averaged vertical plane of symmetry. Cooling further, the CMe group resonances broaden but do not disappear in the baseline, so oscillation

of the N-mesityl groups is not slow enough to remove the mirror plane generating a complex with C_1 symmetry.[43]
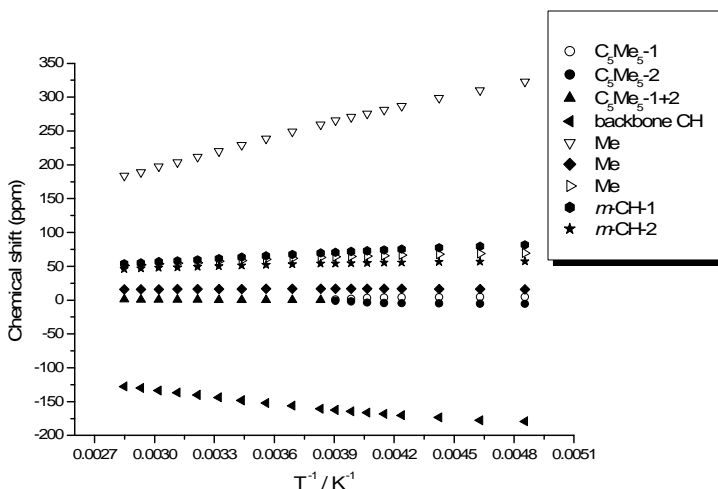

Figure 8. Chemical shift (δ) vs. T^{-1} plot of the ^{1}H NMR resonances of $(C_5Me_5)_2Yb(dad(H)\text{-mesityl})$ in toluene-d_8 at temperatures from −65 to +80°C.

The variable temperature ^{1}H NMR spectra of $(C_5Me_5)_2Yb(dad(Me)\text{-}p\text{-anisyl})$ are similar to $(C_5Me_5)_2Yb(dad(H)\text{-}p\text{-tolyl})$ and $(C_5Me_5)_2Yb(dad(H)\text{-}p\text{-anisyl})$; complete δ vs. T^{-1} plots are in Supporting Information, and the plots for the backbone CH and CMe resonances are shown in Figure 9. The plot shows that the backbone CMe resonance has a strikingly large temperature dependence; it changes from δ +150 (-70 °C) to −50 ppm (+90 °C). The slope is negative, in contrast to the backbone CH resonance in $(C_5Me_5)_2Yb(dad(H)\text{-}p\text{-tolyl})$, which is positive, as shown in Figure 9. The different sign of the slope in the δ vs. T^{-1} plot is expected when a methyl group replaces a hydrogen atom at a given site in a paramagnetic molecule when the Fermi contact term dominates the pseudo-contact term, since the hyperfine coupling constant a_H and a_{Me} have different signs.[31] Similarly, the change of sign of the slope in the δ vs. T^{-1} plot was observed in $(C_5Me_5)_2Yb(bipy\text{-}X)$, when the X-substituents in the 4,4'-sites are changed from H to Me.[3]

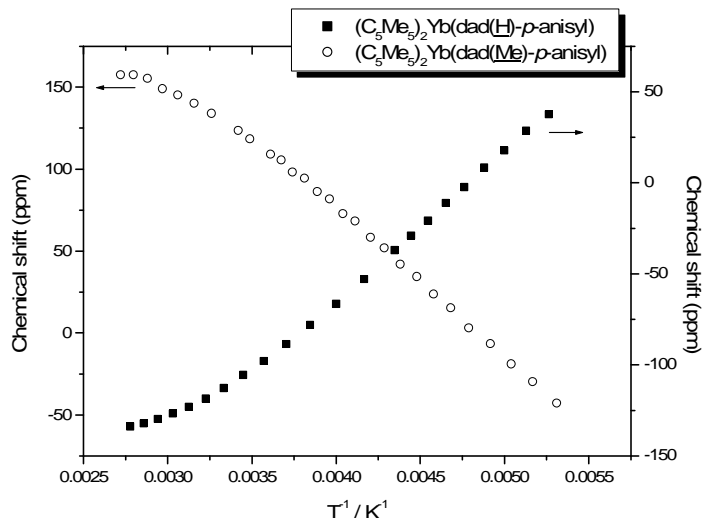**Figure 9.** Chemical shift (δ) vs. T^{-1} plot of the ^{1}H NMR backbone CH/CMe resonances of $(C_5Me_5)_2Yb(dad(H)-p$-anisyl$)$ and $(C_5Me_5)_2Yb(dad(Me)-p$-anisyl$)$ in toluene-d_8 at temperatures from -70 to +90°C.

(c) The Alkyl Substituted Complexes, $(C_5Me_5)_2Yb(dad(H)-R)$, R= alkyl.

In general, the pattern of chemical shifts in the alkyl-substituted complexes are similar to those of the aryl ones, with one notable exception, *viz.*, when R= *t*-Bu. In this case, the resonance due to the CMe_3 groups are not observed at 20 °C in C_6D_6 or C_7D_8. However, as shown in the δ vs. T^{-1} plot in Figure 10, the resonances due to the CMe_3 groups are observed at 95 °C ($T^{-1} = 0.0027$ K^{-1}) as a broad singlet that disappears into the baseline as the temperature is reduced below 80 °C, then emerge from the baseline as two widely separated resonances at δ= 9.6 and 119 ppm in a 2:1 ratio, respectively. The chemical shift of the decoalesced resonances are then independent of temperature. This temperature behavior is presumably due to hindered rotation around the N-CMe_3 bond that is slow on the NMR time scale below 250 K, resulting from steric hindrance between the CMe_3 groups and the CMe groups on the C_5Me_5 rings. Two complexes, $(C_5H_5)_2Yb(dad(H)-t$-Bu$)$[11] and $(C_5Me_4H)_2Yb(dad(H)-t$-Bu$)$, are prepared and

20

characterized as detailed in the Experimental Section and Table 2 in order to examine the effect of cyclopentadienyl ring substituents on the rotation barrier.
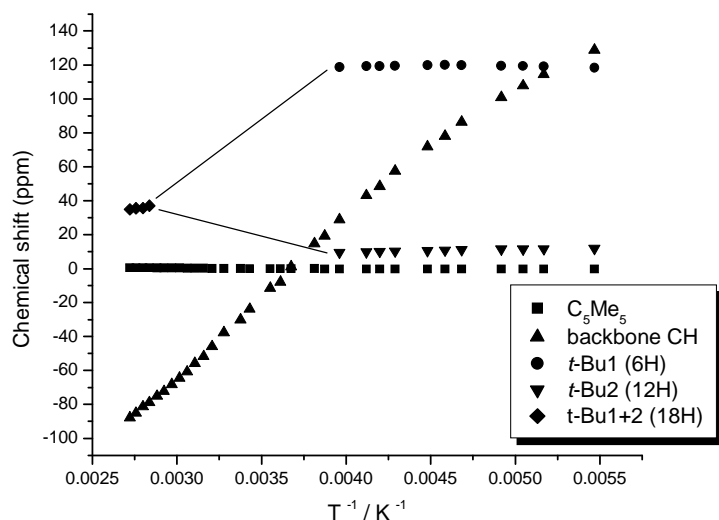

Figure 10. Chemical shift (δ) vs. T^{-1} plot of the ^1H NMR resonances of $(C_5Me_5)_2Yb(dad(H)$-t-Bu) in toluene-d_8 at temperatures from -70 to +90°C.
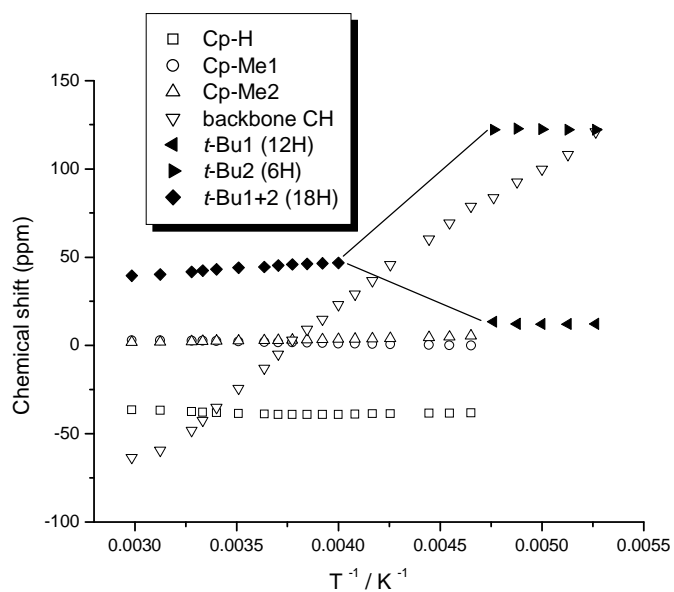
Figure 11. Chemical shift (δ) vs. T^{-1} plot of the ^1H NMR resonances of $(Me_4C_5H)_2Yb(dad(H)\text{-}tBu)$ in toluene-d_8 at temperatures from -70 to +90°C.

Figure 11 shows the resonances of the C_5Me_4H derivative as a δ vs. T^{-1} plot, which is similar to that of $(C_5Me_5)_2Yb(dad(H)\text{-}t\text{-}Bu)$, Figure 10, with the exception of the temperature at which the CMe_3 resonances disappear into and reappear from the baseline. In the C_5Me_4H metallocene, the coalescence temperature is about 35 °C lower than that for the C_5Me_5 derivative, consistent with less steric hindrance to rotation. In addition, the CMe_3 resonance is a single resonance down to -70 °C in $(C_5H_5)_2Yb(dad(H)\text{-}t\text{-}Bu)$; the δ vs. T^{-1} plot is available as Supporting Information.

The temperature dependence of the resonances of $(C_5Me_5)_2Yb(dad(H)\text{-}i\text{-}Pr)$, Figure 12, shows that the CH*Me₂* resonances do not decoalesce to -70 °C, which is also consistent with the steric hindrance to rotation postulate. The variable temperature spectra of $(C_5Me_5)_2Yb(dad(H)\text{-}i\text{-}Pr)$ contain additional information since the slope of the δ vs. T^{-1} plot for the CH and CMe_2 resonances have opposite signs. As mentioned above, this is the expected behavior, when the Fermi contact term dominates the pseudo-contact term.[31] This behavior shows that the unpaired spin density is delocalized onto the methyl groups, presumably by hyperconjugation, consistent with an electronic component to the N-C rotation barrier. It is noteworthy that the EPR spectrum of $[dad(H)\text{-}t\text{-}Bu]^{\bullet-}$ shows unpaired spin density on the CMe_3 groups,[44] which was attributed to hyperconjugation. Thus, NMR and EPR spectra support the idea of an electronic contribution to the N-C(R) rotation barrier, however steric hindrance to rotation is likely to be the major contributor.[45]
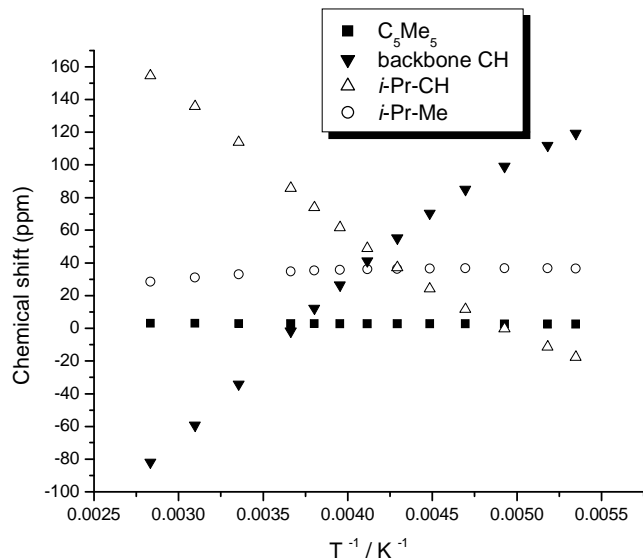
Figure 12. Chemical shift (δ) vs. T^{-1} plot of the ^{1}H NMR resonances of $(C_5Me_5)_2Yb(dad(H)-i\text{-}Pr)$ in toluene-d_8 at temperatures from -70 to +90°C.

(d) Quantitative Evaluation of the N-CMe₃ Rotation Barrier

The rotation barriers in the dad(H)-R, where R is aryl, listed in Table 6, are readily obtained since they involve coalescence of two resonances of equal intensity.[40-42] This graphical method cannot be used, however, for estimating the free energy barrier in the dad(H)-t-Bu complexes since the populations of the exchanging sites are unequal. In a diamagnetic compound, line-shape analysis is used to solve this problem, but this method requires that the spin-spin relaxation time (T_2) does not depend on temperature, a condition that is not valid for paramagnetic compounds, whose line-widths often are very temperature dependent. An analytical method, however, has been developed for estimating the activation free energies for a 2:1 site exchange.[46] This method is outlined in the Experimental Section, and the values obtained for the activation energies given in Table 7 are reasonable as they are similar to those in Table 6.

Table 7. Barrier to CMe₃ site exchange in Cp'₂Yb(dad(H)-t-Bu)

	$(C_5Me_5)_2Yb(dad(H)-t-Bu)$	$(Me_4C_5H)_2Yb(dad(H)-t-Bu)$
$\Delta\nu$ [Hz] [a]	~ 50000	~ 54500
T_c [K] [b]	~ 345	~ 235
$\Delta G_A^{\ddagger}$ [kcal mol^{-1}] [c]	13	9
$\Delta G_B^{\ddagger}$ [kcal mol^{-1}] [c]	12	8

[a] distance between the signals in Hz

[b] T_c = coalescence temperature [400 MHz operating frequency]

[c] As T_c and $\Delta\nu$ are determined by an extrapolation of the temperature dependence of the CMe_3 protons in C_7D_8 as described in the Experimental Section. The free energy of activation, $\Delta G^{\ddagger}$, is given without specifying the uncertainty in the value.

The relative barriers are consistent with steric hindrance playing a large role in the barrier. However, the X-ray crystal structure of $(C_5Me_5)_2Yb(dad(H)-t-Bu)$ and $(C_5H_5)_2Yb(dad(H)-t-Bu)$ do not show short intramolecular distances, though the Yb-N(ave.) distance in $(C_5Me_5)_2Yb(dad(H)-t-Bu)$ of 2.390(2) Å is significantly longer than the equivalent distance in the C_5H_5-complex of 2.306(9) Å.[11, 12] The representation of the crystal structure of the former complex by van der Waals spheres shows that the CMe_3 groups and C_5Me_5 rings are interlocking (see Supporting Information for this representation). Unfortunately, the chemically inequivalent methyl resonances in the less sterically congested complex, $(C_5Me_4H)_2Yb(dad(H)-t-Bu)$, just disappear into the baseline and the C_5Me_4H rotation barrier cannot be estimated.

While the work described in this paper was in progress, the synthesis and crystal structure of $(C_5Me_5)_2Yb(dad(H)-t-Bu)$ was published,[12] however, the reported ^1H NMR spectrum is different from ours. The cell dimensions of our complex agree with those reported, see Experimental Section for details, showing that the solids are identical. Trifonov et al. report that the CMe_3 resonances appear as four unequal area resonances (δ -6.7, 12.2, 19.2 and 24.2 ppm) at 20 °C in C_6D_6 whereas we do not observe these resonances under the same conditions, Figure 13. We noted, however, that when our material is allowed to stand at room temperature in an NMR tube that is sealed with a rubber septum, resonances appear at the chemical shifts reported by Trifonov et al., suggesting that the reported

24

resonances are due to decomposition products. In a sealed NMR tube, $(C_5Me_5)_2Yb(dad(H)-t-Bu)$ is indefinitely stable in C_6D_6 at 20 °C. Trifonov et al. also report that thf-d_8 displaces dad(H)-t-Bu giving $(C_5Me_5)_2Yb(thf)_x$.[12] We have reproduced this observation with neat thf-d_8, however, addition of a drop of thf-d_8 to a solution of $(C_5Me_5)_2Yb(dad(H)-t-Bu)$ in C_6D_6 does not perturb the ^{1}H NMR chemical shifts at 20 °C. In contrast, $(C_5Me_5)_2Yb(dad(H)-p-tolyl)$ does not exchange with neat thf-d_8, since the resonances in that solvent are identical to those obtained in C_6D_6 at 20 °C. 2,2'-Bipyridine displaces the diazabutadiene ligand in $(C_5Me_5)_2Yb(dad(H)-t-Bu)$ on mixing giving $(C_5Me_5)_2Yb(bipy)$ and free dad(H)-t-Bu; the reverse reaction does not occur, clearly showing the relative thermodynamic stability of the bipy complex.[1] As reported, free bipy does not exchange with $(C_5Me_5)_2Yb(bipy)$ on the NMR time scale, however it does exchange with 4,4'-dimethyl-2,2'-bipyridine on the chemical time scale.[1] These, and other recently reported exchange studies,[47, 48] show that the mechanism of ligand exchange also involves a redox process.
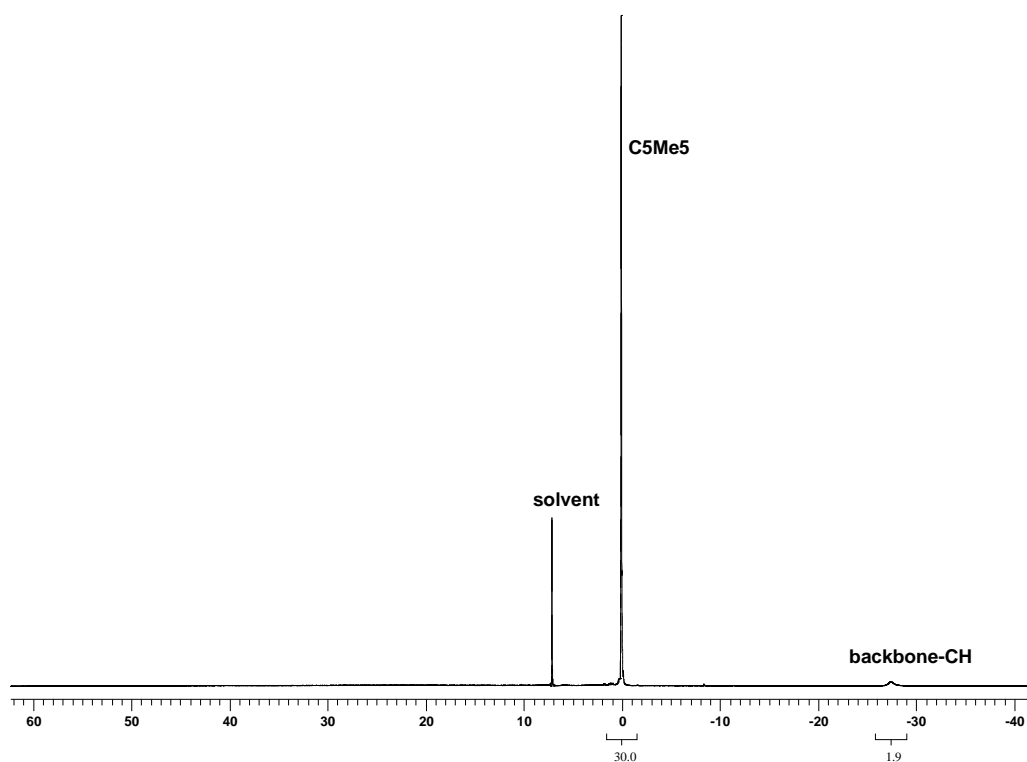

Figure 13. ^{1}H NMR spectrum of $(C_5Me_5)_2Yb(dad(H)-t-Bu)$ in benzene-d_6 at 20 °C.

(e) Relation Between Solid and Solution State Magnetism

Figures 14a and 14b show plots of the solid state magnetic susceptibility, expressed as χT, vs. the reduced observed chemical shift of the backbone CH/CMe resonance in the solution ^{1}H NMR spectrum, expressed as ϑ_{298}, for several dad(R')-R complexes. The reduced chemical shift (ϑ_{298}) is defined as the observed chemical shift at a given temperature multiplied by that temperature, δT divided by 298 K. These graphs dramatically illustrate the linear relation between solution and solid state magnetic properties and show that the observed magnetic properties result from the individual molecule not from the collection of molecules in the ensemble. This implies that the phenomena responsible for the non-linear behavior in the individual χT vs. T and ϑ_{298} vs. T plots are traceable to the magnetic properties of the individual molecular complexes, and therefore to the energy and overlap of the molecular orbitals.

The origin of the slight curvature at low temperature (-60 to -70 °C) in Figure 14b, but not in Figure 14a, parallels the non-linear chemical shift behavior of the backbone-H over a similar temperature range observed for the alkyl derivatives in Figures 10 and 12, S11 and S15 (see Supporting Information), that is not compensated by changes in χT (in the solid state). Since all processes are intramolecular in solution, the non-linearity might be due to slowing of some dynamical process, such as motion of the N-heterocyclic ligand about the horizontal mirror plane, that does not occur in the solid state in this temperature regime.
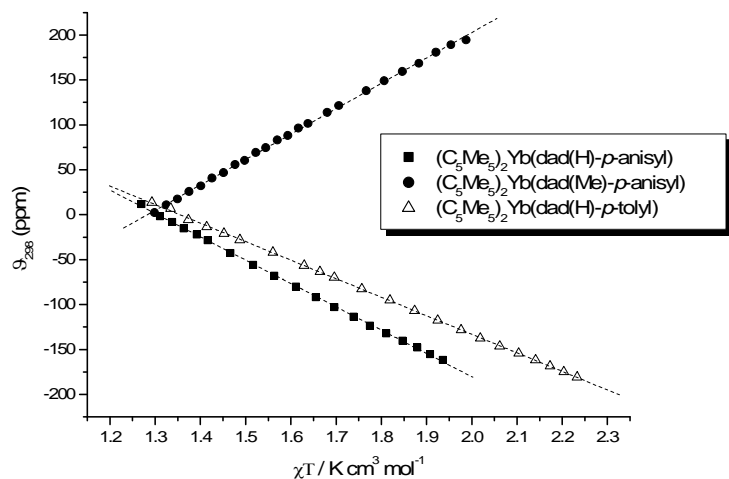
Figure 14a. Reduced observed chemical shift (ϑ_{298}) vs. χT plot of ^{1}H NMR resonances of backbone-R' in $(C_5Me_5)_2Yb(dad(R')$-aryl) systems in toluene-d_8 at temperature from -70°C to +90°C.
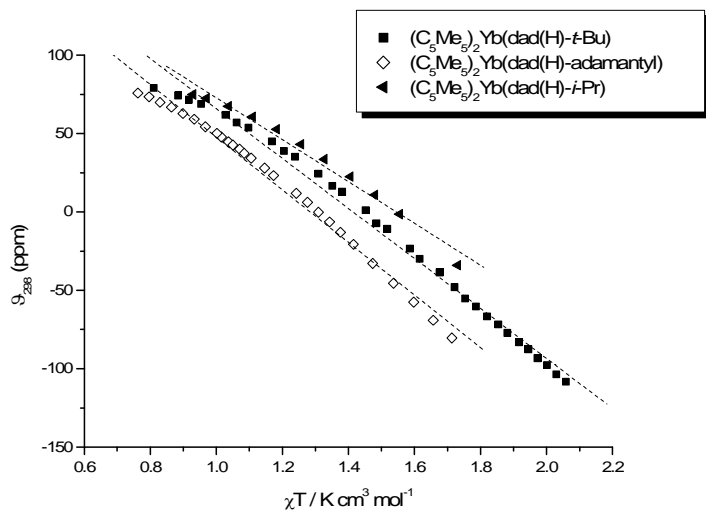
Figure 14b. Reduced observed chemical shift (ϑ_{298}) vs. χT plot of ^{1}H NMR resonances of backbone-R' in $(C_5Me_5)_2Yb(dad(H)$-alkyl) systems in toluene-d_8 at temperatures from -70°C to +90°C.

In an earlier article,[3] a qualitative symmetry orbital model was developed, in which the antiferromagnetic exchange coupling was traced to the interaction between the electron or hole on the

bent sandwich fragment $(C_5Me_5)_2Yb(III, f^{13})$ which is of f- or d-parentage or hybridization therefrom, with the electron in the radical anion in an orbital of b_1-symmetry. This qualitative coupling scheme depends on the relative orbital energies and overlap integrals of the individual fragments and ultimately on the crystal field states of B_1 symmetry on the ytterbocene fragment.

Conclusions

The studies described in this paper, along with those in earlier papers[1-3] show that the bipy-X and dad(R')-R ligands, whose HOMO's have identical symmetry but different energies, form complexes with $(C_5Me_5)_2Yb$ that are not diamagnetic. The extent of paramagnetism in general, as judged by the effective magnetic moment at 300 K, qualitatively correlates with the reduction potential of the ligands. However, the magnetic susceptibility behavior of the individual complexes as a function of temperature is far from simple. This and earlier papers present a phenomenological description of the systematics of the solid state magnetic properties of the ytterbocene complexes with heterocyclic-nitrogen bases, but a molecular level of understanding of the exchange coupling is not possible from these studies. However, a qualitative model is postulated that ascribes the antiferromagnetic coupling to an electron on the $Cp'_2Yb(III)$ fragment of b_1 symmetry with the electron in the b_1-molecular orbital in the ligand radical anion. The tools used by physicists, such as those described in ref. 8, must be employed in order to achieve a molecular level of understanding; these and related studies will be reported in due course.

Experimental Section

General Comments. All reactions, product manipulations, and physical studies have been carried out as previously described.[1-3] The temperatures quoted in the variable temperature NMR are obtained by calibration of the probe, in the specific instrument used, by recording the chemical shift of methanol (low temperature) and ethyleneglycol (high temperature).[42] The 1,4-diazabutadiene ligands were purified by crystallization and/or sublimation prior to use. The $\Delta G^{\ddagger}$ value for an unequal population site exchange system was determined using eqs. 2 and 3.[46] This method has been applied to the spin-

equilibrium in dimethylmanganocene.[38] Eqs. 2 and 3 give the change in free energy of activation for species A and B.

$$\Delta G_A^{\neq} = 4.57 T_c (10.62 + \log \frac{X}{2\pi(1-\Delta p)} + \ln \frac{T_c}{\Delta \nu}) \qquad (2)$$

$$\Delta G_B^{\neq} = 4.57 T_c (10.62 + \log \frac{X}{2\pi(1+\Delta p)} + \ln \frac{T_c}{\Delta \nu}) \qquad (3)$$

The terms in these eqs. are defined by the Graph below, with T_c, the coalescence temperature, $\Delta \nu$, the extrapolated chemical shift difference in Hertz, and the expressions $\log[X/(2\pi(1\pm\Delta p)]$, where $\Delta p = -0.33$ when the population difference is 1:2, are evaluated from Figure 2 in ref. 46. However, the $\Delta G^{\ddagger}$ values obtained in this way are only valid at the coalescence temperature, T_c.[46]
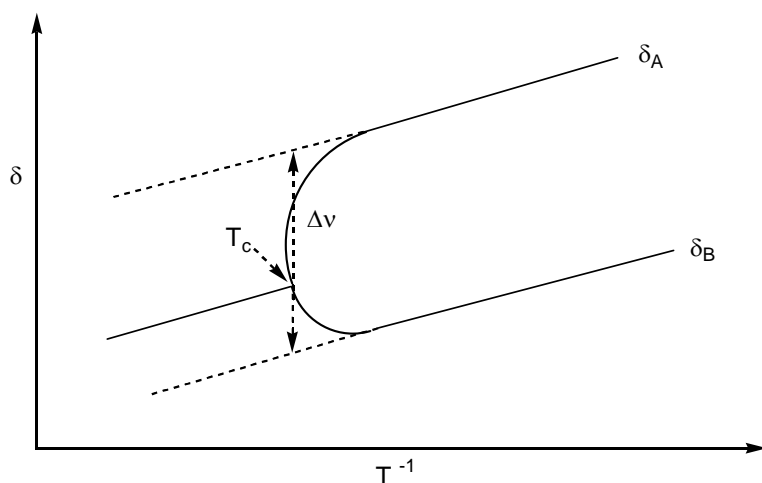
($C_5Me_5)_2$Yb(N,N'-bis(p-tolyl)-1,4-diazabutadiene). N,N'-Bis(p-tolyl)-1,4-diazabutadiene[49] (0.27 g, 1.1 mmol) and ($C_5Me_5)_2$Yb(OEt$_2$)[50] (0.59 g, 1.1 mmol) were weighed into a Schlenk flask under nitrogen, dissolved in toluene (80 mL) and the dark green-black solution was stirred at room temperature for 3 h. The solvent was removed under dynamic vacuum and the residue was sublimed in diffusion pump vacuum at 160-180 °C. The sublimed material was dissolved in ca. 100 mL of pentane, filtered and the filtrate was concentrated and cooled to –25 °C overnight to form dark green crystals (0.58 g, 0.83 mmol, 76 %). M.p. 220 °C (dec.). Anal. Calcd for $C_{36}H_{46}N_2$Yb: C, 64.6; H, 7.02; N, 4.08.

Found: C, 64.2; H, 7.02; N, 4.08. ^{1}H NMR (C_6D_6, 20°C): δ 58.3 (6 H, $\nu_{1/2}$ = 90 Hz, *p*-Me), 50.2 (4 H, $\nu_{1/2}$ = 700 Hz, *meta*-CH), 1.74 (30 H, $\nu_{1/2}$ = 55 Hz, C_5Me_5), -123.7 (2H, $\nu_{1/2}$ = 330 Hz, backbone dad-CH). The *ortho*-CH was not observed at 20 °C in C_6D_6. The E.I. mass spectrum showed a molecular ion at m/e= 680 amu. The parent ion isotopic cluster was simulated: (calcd. %, observd. %): 676 (11,11), 677 (41,40), 678 (72,72), 679 (71,70), 680 (100,100), 681 (36,37), 682 (42,42), 683 (15,15), 684 (3,3). IR (Nujol mull; CsI windows; cm^{-1}): 2720 (w), 1604 (vs), 1553 (m), 1497 (vs), 1328 (s), 1313 (sh. w), 1274 (vs), 1181 (m), 1143 (s), 1113 (vw), 1026 (m), 1000 (m), 897 (br. s), 830 (vw), 796 (s), 722 (w), 700 (vw), 647 (vw), 616 (vw), 591 (vw), 513 (m), 415 (br. w), 384 (br. w), 313 (vs), 303 (vs).

($C_5Me_5)_2$Yb(N,N'-bis(*i*-propyl)-1,4-diazabutadiene). N,N'-Bis(*i*-propyl)-1,4-diazabutadiene[51] (0.21 g, 1.5 mmol) and ($C_5Me_5)_2$Yb(OEt$_2$) (0.78 g, 1.5 mmol) were weighed into a Schlenk flask under nitrogen, dissolved in toluene (80 mL) and the bright red solution was stirred at room temperature for 3 h. The solvent was removed under dynamic vacuum and the residue was sublimed in diffusion pump vacuum at 100-120 °C. The sublimed material was dissolved in a minimum amount of pentane (ca. 5 mL) and cooled to –80 °C for several days. The compound crystallized as big, deep red blocks (0.48 g, 0.82 mmol, 55 %), and it was very soluble in aromatic and aliphatic hydrocarbons. M.p. 208-211 °C (dec.). Anal. Calcd for $C_{28}H_{46}N_2Yb$: C, 57.50; H, 7.93; N, 4.79. Found: C, 57.55; H, 8.04; N, 4.74. ^{1}H NMR (C_6D_6, 20°C): δ 108.9 (2 H, $\nu_{1/2}$ = 260 Hz, C*H*Me$_2$), 32.3 (12 H, $\nu_{1/2}$ = 12 Hz, CH*Me*$_2$), 2.83 (30 H, $\nu_{1/2}$ = 9 Hz, C_5Me_5), –28.3 (2H, $\nu_{1/2}$ = 170 Hz, backbone dad-CH). The E.I. mass spectrum showed a molecular ion at m/e= 584 amu. The parent ion isotopic cluster was simulated: (calcd. %, observd. %): 580 (11,10), 581 (43,42), 582 (72,75), 583 (68,66), 584 (100,100). 585 (29,30), 586 (41,36), 587 (13,12). IR (Nujol mull; CsI windows; cm^{-1}): 2720 (w), 1575 (w), 1548 (w), 1338 (w), 1310 (br. w), 1262 (m), 1232 (m), 1160 (m), 1105 (m), 1021 (br. m), 800 (br. m), 784 (m), 720 (br. m), 610 (vw), 475 (vw), 450 (vw), 395 (br. vw), 295 (br. s).

($C_5Me_5)_2$Yb(N,N'-bis(*t*-butyl)-1,4-diazabutadiene). N,N'-Bis(*t*-butyl)-1,4-diazabutadiene[52] (0.23 g, 1.37 mmol) and ($C_5Me_5)_2$Yb(OEt$_2$) (0.71 g, 1.37 mmol) were weighed into a Schlenk flask under nitrogen, dissolved in toluene (80 mL) and the dark red solution was stirred at room temperature for 3 h.

The solvent was removed under dynamic vacuum and the residue was sublimed in diffusion pump vacuum at 180-190 °C. The sublimed material was dissolved in a minimum amount of pentane and cooled to –80 °C for several days. The compound crystallized as deep red blocks (0.45 g, 0.74 mmol, 54 %). M.p. 220-222 °C (dec.). Anal. Calcd for $C_{30}H_{50}N_2Yb$: C, 58.90; H, 8.24; N, 4.58. Found: C, 58.70; H, 8.14; N, 4.63. ^{1}H NMR (C_6D_6, 20°C): δ 0.15 (30 H, $\nu_{1/2}$ = 8 Hz, C_5Me_5), –26.6 (2H, $\nu_{1/2}$ = 200 Hz, backbone dad-CH). The resonance due to the *t*-Bu-protons was not observed at room temperature. The E.I. mass spectrum showed a molecular ion at m/e= 612 amu. The parent ion isotopic cluster was simulated: (calcd. %, observd. %): 608 (11,10), 609 (42,42), 610 (72,75), 611 (68,66), 612 (100,100). 613 (31,30), 614 (41,37), 615 (13,12), 616 (2,2). IR (Nujol mull; CsI windows; cm^{-1}): 2720 (w), 1542 (w), 1492 (m), 1389 (sh), 1368 (s), 1358 (m), 1263 (s), 1220 (w), 1188 (br. vs), 1118 (vw), 1100 (w), 1020 (br. m), 990 (m), 895 (m), 800 (m), 782 (m), 760 (w), 721 (m), 612 (br. w), 532 (vw), 478 (br. m), 383 (br. m), 280 (br. vs). Unit cell determination of $(C_5Me_5)_2Yb(dad(H)$-*t*-Bu): A crystal measuring 0.12 x 0.20 x 0.22 mm was mounted on a glass fiber using Paratone N hydrocarbon oil, and transferred to a Bruker SMART 1k CCD diffractometer. Cell constants and an orientation matrix were obtained of the measured positions of reflections with I > 10σ to give the following unit cell: *a*= 13.7007(29) Å, *b*= 15.5126(13) Å, *c*= 13.3171(18) Å, α= β= γ= 90 °. These values are in agreement with the reported values in the orthorhombic space group Pna2$_1$: *a*= 13.7169(1) Å, *b*= 15.5660(2) Å, *c*= 13.3681(2) Å, α= β= γ= 90 °.[12]

$(C_5Me_5)_2Yb(N,N'$-bis(*p*-anisyl)-1,4-diazabutadiene). N,N'-Bis(*p*-anisyl)-1,4-diazabutadiene[49] (0.33 g, 0.99 mmol) and $(C_5Me_5)_2Yb(OEt_2)$ (0.51 g, 0.99 mmol) were weighed into a Schlenk flask under nitrogen, dissolved in toluene (80 mL) and the dark green-black solution was stirred at room temperature for 1 h. The solvent was removed under dynamic vacuum and the residue was sublimed in diffusion pump vacuum at 200-220 °C. The sublimed material was dissolved in ca. 100 mL of pentane, filtered and the filtrate was concentrated and cooled to –25 °C overnight to form dark green shiny plates (0.45 g, 0.63 mmol, 64 %). M.p. 260-262 °C (dec.). Anal. Calcd for $C_{36}H_{46}N_2O_2Yb$: C, 60.75; H, 6.51;

N, 3.94. Found: C, 60.60; H, 6.56; N, 4.21. ^{1}H NMR (C$_6$D$_6$, 20°C): δ 46.9 (4 H, $\nu_{1/2}$ = 350 Hz, *meta*-CH), 18.9 (6 H, $\nu_{1/2}$ = 4 Hz, *p*-OMe), 1.76 (30 H, $\nu_{1/2}$ = 13 Hz, C$_5$Me$_5$), -109.3 (2H, $\nu_{1/2}$ = 270 Hz, backbone dad-CH). The *ortho*-CH was not observed at 20 °C in C$_6$D$_6$. The E.I. mass spectrum showed a molecular ion at m/e= 712 amu. The parent ion isotopic cluster was simulated: (calcd. %, observd. %): 708 (10,10), 709 (41,40), 710 (72,72), 711 (70,70), 712 (100,100). 713 (37,37), 714 (42,42), 715 (16,16), 716 (3,3). IR (Nujol mull; CsI windows; cm^{-1}): 2720 (vw), 1602 (m), 1570 (br. w), 1503 (vs), 1300 (m), 1278 (s), 1250 (vs), 1188 (w), 1172 (m), 1112 (sh), 1098 (br. m), 1052 (br. m), 822 (m), 800 (m), 780 (m), 722 (br. w), 673 (br. w), 638 (vw), 562 (vw), 532 (w), 510 (vw), 480 (vw), 388 (w), 308 (br. s).

[(C$_5$Me$_5$)$_2$Yb(N,N'-bis(*p*-anisyl)-2,3-dimethyl-1,4-diazabutadiene)]. N,N'-Bis(*p*-anisyl)-2,3-dimethyl-1,4-diazabutadiene[53] (0.29 g, 0.98 mmol) and (C$_5$Me$_5$)$_2$Yb(OEt$_2$) (0.52 g, 1.00 mmol) were weighed into a Schlenk flask under nitrogen, dissolved in toluene (80 mL) and the dark green-brown solution was stirred at room temperature for 1 h. The solvent was removed under dynamic vacuum and the residue was sublimed in diffusion pump vacuum at 170-185 °C. The sublimed material was dissolved in ca. 100 mL of pentane, filtered and the filtrate was concentrated and cooled to –25 °C overnight to form dark green-brown crystals (0.4 g, 0.54 mmol, 55 %). M.p. 219-221 °C (rev.). Anal. Calcd for C$_{38}$H$_{50}$N$_2$O$_2$Yb: C, 61.69; H, 6.81; N, 3.79. Found: C, 61.48; H, 6.75; N, 3.66. ^{1}H NMR (C$_6$D$_6$, 20°C): δ 126.0 (6H, $\nu_{1/2}$ = 360 Hz, backbone dad-C*Me*), 103.3 (4 H, $\nu_{1/2}$ = 800 Hz, *ortho*-CH), 50.1 (4 H, $\nu_{1/2}$ = 34 Hz, *meta*-CH), 18.5 (6 H, $\nu_{1/2}$= 8 Hz, *p*-OMe), 1.51 (30 H, $\nu_{1/2}$ = 23 Hz, C$_5$Me$_5$). The E.I. mass spectrum showed a molecular ion at m/e= 740 amu. The parent ion isotopic cluster was simulated: (calcd. %, observd. %): 736 (11,11), 737 (47,46), 738 (72,72), 739 (71,70), 740 (100,100). 741 (38,40), 742 (42,42), 743 (16,16), 744 (3,3). IR (Nujol mull; CsI windows; cm^{-1}): 2720 (vw), 1603 (w), 1560 (vw), 1555 (w), 1540 (w), 1500 (vs), 1350 (m), 1300 (m), 1290 (m), 1240 (br. vs), 1210 (sh), 1180 (w), 1170 (w), 1105 (br. w), 1038 (sh), 1028 (s), 980 (w), 870 (br. vw), 838 (m), 820 (w), 800 (br. m), 778 (vw), 762 (vw), 710 (br. w), 652 (w), 628 (w), 530 (w), 480 (vbr. w), 390 (vbr. w), 295 (br. s), 275 (sh), 245 (m).

(C$_5$Me$_5$)$_2$Yb(N,N'-bis(adamantyl)-1,4-diazabutadiene). N,N'-Bis(adamantyl)-1,4-diazabutadiene[54] (0.33 g, 1.01 mmol) and (C$_5$Me$_5$)$_2$Yb(OEt$_2$) (0.53 g, 1.02 mmol) were weighed into a Schlenk flask under nitrogen, dissolved in toluene (120 mL) and the dark red solution was stirred at room temperature for 2 h. The solution was filtered, concentrated to *ca.* 50 ml and cooled to –25 °C overnight to form brown-red crystals (0.62 g, 0.80 mmol, 79 %). M.p. 238–239 °C (rev.). Anal. Calcd for C$_{42}$H$_{62}$N$_2$Yb: C, 65.68; H, 8.14; N, 3.65. Found: C, 65.51; H, 8.31; N, 3.69. ^{1}H NMR (C$_6$D$_6$, 20°C): δ 18.9 (2H, $\nu_{1/2}$ ~ 650 Hz, adamantyl-CH$_2$), 16.7 (6 H, $\nu_{1/2}$ ~ 400 Hz, adamantyl-CH$_2$), 12.5 (7H, $\nu_{1/2}$ = 67 Hz, adamantyl-CH), 0.14 (30 H, $\nu_{1/2}$ = 8 Hz, C$_5$Me$_5$), -25.2 (2H, $\nu_{1/2}$ = 200 Hz, backbone dad-CH). IR (Nujol mull; CsI windows; cm^{-1}): 2720 (vw), 2670 (vw), 2650 (vw), 1622 (br. w), 1482 (m), 1352 (m), 1341 (m), 1312 (m), 1303 (m), 1272 (m), 1234 (vs), 1185 (m), 1178 (m), 1112 (m), 1185 (w), 1178 (m), 1112 (m), 1088 (vs), 1069 (m), 1012 (br. m), 995 (w), 980 (vw), 970 (vw), 954 (w), 938 (w), 912 (m), 812 (br. m), 775 (s), 721 (m), 698 (vw), 620 (br. w), 470 (br. m), 418 (br. m), 380 (br. w), 355 (br. w), 280 (br. vs), 245 (w), 221(m).

(C$_5$Me$_5$)$_2$Yb(N,N'-bis(mesityl)-1,4-diazabutadiene). N,N'-Bis(mesityl)-1,4-diazabutadiene[55] (0.44 g, 1.5 mmol) and (C$_5$Me$_5$)$_2$Yb(OEt$_2$) (0.78 g, 1.5 mmol) were weighed into a Schlenk flask under nitrogen, dissolved in toluene (80 mL) and the green-blue solution was stirred at room temperature for 3 h. The solution was filtered, concentrated and cooled to –25 °C overnight. The compound crystallized in dark blue-green crystals (0.52 g, 0.71 mmol, 47 %), and it was nearly insoluble in aliphatic hydrocarbons and moderately soluble in aromatic hydrocarbons. M.p. 230-232 °C (dec.). Anal. Calcd for C$_{40}$H$_{54}$N$_2$Yb: C, 65.28; H, 7.40; N, 3.81. Found: C, 65.55; H, 7.37; N, 3.98. ^{1}H NMR (C$_6$D$_6$, 20°C): δ 224.9 (6 H, $\nu_{1/2}$ = 120 Hz, mesityl-Me), 62.5 (2 H, $\nu_{1/2}$ = 32 Hz, mesityl-CH), 58.2 (6 H, $\nu_{1/2}$ = 24 Hz, mesityl-Me), 50.4 (2 H, $\nu_{1/2}$ = 24 Hz, mesityl-CH), 16.6 (6 H, $\nu_{1/2}$ = 35 Hz, mesityl-Me), 0.29 (30 H, $\nu_{1/2}$=90 Hz, C$_5$Me$_5$), −146.2 (2H, $\nu_{1/2}$ = 240 Hz, backbone dad-CH).

(C$_5$Me$_4$H)$_2$Yb(N,N'-bis(*t*-butyl)-1,4-diazabutadiene). N,N'-Bis(*t*-butyl)-1,4-diazabutadiene[52] (0.085 g, 0.51 mmol) and (C$_5$HMe$_4$)$_2$Yb(OEt$_2$)[42] (0.25 g, 0.51 mmol) were weighed into a Schlenk flask under

nitrogen, dissolved in toluene (80 mL) and the bright red solution was stirred at room temperature for 2 h. The solvent was removed under dynamic vacuum and the residue was sublimed in diffusion pump vacuum at 180-190 °C to give analytically and spectroscopically pure product as red crystalline material (0.18 g, 0.31 mmol, 60 %). M.p. 242-245 °C (dec.). Anal. Calcd for $C_{28}H_{46}N_2Yb$: C, 57.61; H, 7.94; N, 4.80. Found: C, 57.31; H, 8.00; N, 4.72. ^{1}H NMR (C_6D_6, 20°C): δ 43.1 (18 H, $v_{1/2}$ = 480 Hz, dad-CMe_3), 2.62 (12 H, $v_{1/2}$ = 30 Hz, C_5HMe_4), 2.47 (12 H, $v_{1/2}$ = 50 Hz, C_5HMe_4), −36.0 (2H, $v_{1/2}$ = 180 Hz, backbone dad-CH), −38.0 (2H, $v_{1/2}$ = 60 Hz, C_5HMe_5). The E.I. mass spectrum showed a molecular ion at m/e= 584 amu. The parent ion isotopic cluster was simulated: (calcd. %, observd. %): 580 (12,11), 581 (43,42), 582 (73,74), 584 (100,100), 585 (29,29), 586 (41,41), 587 (13,14), 588 (2,2).

Supporting Information Available. Crystallographic data, labeling diagrams, tables giving atomic positions, anisotropic thermal parameters, bond distances, bond angles, torsion angles, least square planes, and packing diagrams. The representation of (C_5Me_5)$_2$Yb(dad(H)-*t*-Bu) as van der Waals representation is also available as are χT vs. T, observed chemical shift δ vs. T^{-1}, reduced observed chemical shift (ϑ_{298}) and reduced isotropic chemical shift (ϑ_{298}^{iso}) vs. T plots referred to in the text. This material is available free of charge via the Internet at http://pubs.acs.org. Structure factor tables are available from the authors. Crystallographic data were also deposited with Cambridge Crystallographic Data Centre. Copies of the data (CCDC 615276 & 615277) can be obtained free of charge via http://www.ccdc.cam.ac.uk/data_request/cif by e-mailing data_request@ccdc.cam.ac.uk, or by

contacting The Cambridge Crystallographic Data Centre, 12, Union Road, Cambridge CB 1EZ, UK; fax +44 1223 336033.

References

[1]   Schultz, M.; Boncella, J. M.; Berg, D. J.; Tilley, T. D.; Andersen, R. A., *Organometallics* **2002,** *21*, 460-472.

[2]   Walter, M. D.; Schultz, M.; Andersen, R. A., *New J. Chem.* **2006,** *30*, 238-246.

[3]   Walter, M. D.; Berg, D. J.; Andersen, R. A., *Organometallics* **2006,** *25*, 3228-3237.

[4]   Berg, D. J.; Boncella, J. M.; Andersen, R. A., *Organometallics* **2002,** *21*, 4622-4631.

[5]   Rosen, R. K.; Andersen, R. A.; Edelstein, N. M., *J. Am. Chem. Soc.* **1990,** *112*, 4588-4590.

[6]   Veauthier, J. M.; Schelter, E. J.; Kuehl, C. J.; Clark, A. E.; Scott, B. L.; Morris, D. E.; Martin, R. L.; Thompson, J. D.; Kiplinger, J. L.; John, K. D., *Inorg. Chem.* **2005,** *44*, 5911-5920.

[7]   Kuehl, C. J.; Da Re, R. E.; Scott, B. L.; Morris, D. E.; John, K. D., *Chem. Commun.* **2003**, 2336-2337.

[8]   Booth, C. H.; Walter, M. D.; Daniel, M.; Lukens, W. W.; Andersen, R. A., *Phys. Rev. Lett.* **2005,** *95*, 267202.

[9]   Recknagel, A.; Noltemeyer, M.; Edelmann, F. T., *J. Organomet. Chem.* **1991,** *410*, 53-61.

[10] Moore, J. A.; Cowley, A. H.; Gordon, J. C., *Organometallics* **2006**, *25*, 5207-5209.

[11] Trifonov, A. A.; Kirillov, E. N.; Bochkarev, M. N.; Schumann, H.; Muehle, S., *Russ. Chem. Bull.* **1999,** *48*, 381-384.

[12] Trifonov, A. A.; Kurskii, Y. A.; Bochkarev, M. N.; Muehle, S.; Dechert, S.; Schumann, H., *Russ. Chem. Bull.* **2003,** *52*, 601-606.

[13] Trifonov, A. A.; Fedorova, E. A.; Ikorskii, V. N.; Kurskii, Y. A.; Dechert, S.; Schumann, H.; Bochkarev, M. N., *Eur. J. Inorg. Chem.* **2005**, 2812-2818.

[14] Trifonov, A. A.; Kirillov, E. N.; Dechert, S.; Schumann, H.; Bochkarev, M. N., *Eur. J. Inorg. Chem.* **2001**, 2509-2514.

[15] Trifonov, A. A.; Fedorova, E. A.; Fukin, G. K.; Druzhkov, N. O.; Bochkarev, M. N., *Angew. Chem.* **2004,** *116*, 5155-5158.

[16] Trifonov, A. A.; Fedorova, E. A.; Fukin, G. K.; Baranov, E. V.; Druzhkov, N. O.; Bochkarev, M. N., *Chem. Eur. J.* **2006,** *12*, 2752-2757.

[17] McPherson, A. M.; Fieselmann, B. F.; Lichtenberger, D. L.; McPherson, G. L.; Stucky, G. D., *J. Am. Chem. Soc.* **1979,** *101*, 3425-3430.

[18] Kaim, W., *J. Am. Chem. Soc.* **1982,** *104*, 3833-3837.

[19] Kaupp, M.; Stoll, H.; Preuss, H.; Kaim, W.; Stahl, T.; van Koten, G.; Wissing, E.; Smeets, W. J. J.; Spek, A. L., *J. Am. Chem. Soc.* **1991,** *113*, 5606-5618.

[20] Coulombeix, J.; Emmenegger, F.-P., *Helv. Chim. Acta* **1985,** *68*, 248-254.

[21] tom Dieck, H.; Renk, I. W., *Chem. Ber.* **1971,** *104*, 110-130.

[22] van Koten, G.; Vrieze, K., *Adv. Organomet. Chem.* **1982,** *21*, 151-239.

[23] The uncoupled value of 4.85 μ_B is obtained by summing the χT value of each spin carrier; this assumes that all of the crystal field states derived from the $^2F_{7/2}$ term of Yb(III) are populated (see ref. 1).

[24] Tilley, T. D.; Andersen, R. A.; Spencer, B.; Zalkin, A., *Inorg. Chem.* **1982,** *21*, 2647-2649.

[25] Huige, C. J. M.; Spek, A. L.; de Boer, J. L., *Acta Cryst.* **1983,** *C41*, 113-116.

[26] Carlson, C. N.; Kuehl, C. J.; Da Re, R. E.; Veauthier, J. M.; Schelter, E. J.; Milligan, A. E.; Scott, B. L.; Bauer, E. D.; Thompson, J. D.; Morris, D. E.; John, K. D., *J. Am. Chem. Soc.* **2006,** *128*, 7230-7241.

[27] Variable temperature Yb L_{III}-edge XANES studies on the compounds reported here and other bipy-X compounds will be published in due course.(Booth, C.H., personal communication).

[28] The isotropic chemical shifts ($\delta^{iso}= \delta^{obs} - \delta^{dia}$) are not determined, since the diamagnetic analogues to the molecules presented in this paper, e.g. $(C_5Me_5)_2Ca(dad(R')-R)$ have not been prepared. However, approximate isotropic shifts (δ^{iso}) using the chemical shifts of $(C_5Me_5)_2Yb(py)_2$ and the free dad(R')-R ligands have been calculated, see Supporting Information. Errors introduced by non-ideal reference compounds are expected to be small for ^1H NMR data.

[29] Maron, L.; Werkema, E. L.; Perrin, L.; Eisenstein, O.; Andersen, R. A., *J. Am. Chem. Soc.* **2005,** *127*, 279-292.

[30] Zi, G.; Blosch, L. L.; Jia, L.; Andersen, R. A., *Organometallics* **2005,** *24*, 4602-4612.

[31] [a] La Mar, G. N.; Horrocks, W. D.; Holm, R. H., *NMR of Paramagnetic Molecules.* ed.; Academic Press: New York, 1973; pp 85-178. [b] Wicholas, M.; Drago, R. S. *J. Am. Chem. Soc.* **1968**, *90*, 6946-6950. [c] Horrocks, W. D.; Taylor, R. C.; LaMar, G. N. *J. Am. Chem. Soc.* **1964**, *86*, 3031-3038. [d] LaLancette, E. A.; Eaton, D. R.; Benson, R. E.; Phillips, W. D. *J. Am. Chem. Soc.* **1962**, *84*, 3968-3970.

[32] Köhler, F. H., Probing Spin Densities by Use of NMR Spectroscopy. In *Magnetism: Molecules to Materials. Models and Experiments*, ed.; Miller, J. S.; Drillon, M., Eds. Wiley-VCH: Weinheim, 2001; pp 379-430, and references cited therein.

[33] Fischer, R. D., NMR-spectroscopy of organo-f-element and pre-lanthanoid complexes: some current trends. In *Fundamental and Technological Aspects of Organo-f-Element Chemistry*, ed.; Marks, T. J.; Fragalà, I. L., Eds. D. Reidel: Dordrecht, 1985; pp 277-326.

[34] Fischer, R. D., Lanthanide and Actinide Complexes. In *NMR of Paramagnetic Molecules*, ed.; La Mar, G. N.; Horrocks, W. D.; Holm, R. H., Eds. Academic Press: New York, 1973; pp 521-553.

[35] Kurland, R. J.; McGarvey, B. R., *J. Magn. Reson.* **1970,** *2*, 286-301.

[36] Knorr, R.; Polzer, H.; Bischler, E., *J. Am. Chem. Soc.* **1975,** *97*, 643-644.

[37] Knorr, R.; Weiss, A.; Polzer, H.; Bischler, E., *J. Am. Chem. Soc.* **1975,** *97*, 644-646.

[38] Köhler, F. H.; Schlesinger, B., *Inorg. Chem.* **1992,** *31*, 2853-2859.

[39] Heise, H.; Köhler, F. H.; Xie, X., *J. Magn. Reson.* **2001,** *150*, 198-206.

[40] Lukens, W. W.; Beshouri, S. M.; Stuart, A. L.; Andersen, R. A., *Organometallics* **1999,** *18*, 1247-1252.

[41] Luke, W. D.; Streitwieser, A., *J. Am. Chem. Soc.* **1981,** *103*, 3241-3243.

[42] Sandström, J., *Dynamic NMR Spectroscopy*; Academic Press: New York, 1982.

[43] In all the diazabutadiene complexes with $(C_5Me_5)_2Yb$, except the mesityl derivative just discussed, the chemical shift of the C_5Me_5 resonances moves downfield, passes through a minimum value about -50 °C to -60 °C, then moves upfield as the temperature is decreased to -80 °C. This non-linear behavior is due to temperature dependent processes whose populations and chemical shifts depend on temperature.[ref. 32] The averaged chemical shift, δ_{ave}, is the weighted chemical shift of two nuclei, $\delta_{ave} = a\delta_A + b\delta_B$. If the populations are unequal, $a \neq b$, then δ_{ave} vs. T^{-1} will be the sum of the individual δ_A vs. T^{-1} and δ_B vs. T^{-1} plots, which will be non-linear if the populations change with temperature. Conversely, if a=b but $\delta_A \neq \delta_B$, δ_{ave} vs. T^{-1} will be non-linear if δ_A and/or δ_B exhibit non-

linear T^{-1} dependences. Another contributing factor might be the movement of the C_5Me_5 rings relative to the magic angle with temperature, which is related to the $(1-3\cos^2\theta)$ term in the pseudo-contact contribution. The motion of the C_5Me_5 might be correlated to the motion of the N-heterocyclic base about the horizontal mirror plane, however, there is insufficient information in the line shape to delineate the physical process responsible.

[44] Clopath, P.; v. Zelewsky, A., *Helv. Chim. Acta* **1972,** *55*, 52-66.

[45] The low exchange limiting ^{1}H NMR spectrum of $(C_5Me_5)_2Yb(dad(H)\text{-adamantyl})$ could not be reached and the rotation barriers cannot be determined.

[46] Shanan-Atidi, H.; Bar-Elli, K. H., *J. Phys. Chem.* **1970,** *74*, 961-963.

[47] Wang, J.; Amos, R. I. J.; Frey, A. S. P.; Gardiner, M. G.; Cole, M. L.; Junk, P. C., *Organometallics* **2005,** *24*, 2259-2261.

[48] Evans, W. J.; Davis, B. L., *Chem. Rev.* **2002,** *102*, 2119-2136.

[49] Kliegman, J. M.; Barnes, R. K., *J. Org. Chem.* **1970,** *35*, 3140-3143.

[50] Tilley, T. D.; Boncella, J. M.; Berg, D. J.; Burns, C. J.; Andersen, R. A., *Inorg. Synth.* **1990,** *27*, 146-149.

[51] tom Dieck, H.; Franz, K.-D.; Majunke, W., *Z. Naturforsch.* **1975,** *30b*, 922-925.

[52] Kliegman, J. M.; Barnes, R. K., *Tetrahedron* **1970,** *26*, 2555-2560.

[53] tom Dieck, H.; Svoboda, M.; Greiser, T., *Z. Naturforsch.* **1981,** *36b*, 823-832.

[54] Walker, I. Ph.D. Thesis, Eberhard-Karls-Universität, Tübingen, Germany, 2002.

[55] Arduengo, A. J.; Krafczyk, R.; Schmutzler, R.; Craig, H. A.; Goerlich, J. R.; Marshall, W. J.; Unverzagt, M., *Tetrahedron* **1999,** *55*, 14523-14534.